Improvement of Resistance of MgO-Based Refractory to Slag Penetration by *In Situ* Spinel Formation

HUIJUN WANG, BJÖRN GLASER, and DU SICHEN

MgO-*in situ* spinel substrate was prepared at 1773 K (1500 °C) using colloidal alumina suspension and coarse MgO as raw materials. While the addition of 10 mass pct colloidal alumina had limited effect, addition of 20 mass pct colloidal alumina into the MgO matrix improved greatly the resistance of the substrate against the slag penetration at 1873 K (1600 °C). The improvement was found to be mainly related to the formation of solid phases, $CaO{\cdot}Al_2O_3$ and $CaO{\cdot}MgO{\cdot}Al_2O_3$ at the grain boundaries due to slag-spinel reaction. Putting the reacted substrate into contact again with new slag revealed no appreciable new slag penetration. The results showed a potential solution to improve the resistance of MgO-based refractory to slag penetration and to improve steel cleanness.

DOI: 10.1007/s11663-014-0277-7

I. INTRODUCTION

THE role of ladle glaze as an important source of the formation of inclusions has evidently been reported.[1–8] Ladle glaze is formed during the casting process. The top slag adheres to the ladle lining, while it goes down following the steel melt during the draining of the ladle. After the first heat, a decarburized layer is formed on the original MgO-C refractory. The decarburized layer is usually porous. The adhered slag penetrates into the open pores of the refractory. After casting, two layers are found above the decarburized refractory in the wall of a MgO-C lined ladle, *viz*. a slag-infiltrated layer and the outer slag layer. While the outer layer of the glaze would be removed during the filling of the ladle in the next heat, the slag-infiltrated layer would not be easily removed because of the MgO matrix. The movement of the liquid steel near the wall would flush off the tiny particles (droplets) from the slag-infiltrated layer resulting in calcium aluminate inclusions. The slag infiltration followed by flushing off of tiny particles (droplets) from the lining in the next heat is a self-acceleration process. The process would be enhanced when a ladle becomes older (more porous). In order to reduce the number of inclusions introduced by the refractory lining, blocking the pores of the MgO matrices and reducing the slag infiltration are essential.

In situ spinel (magnesia aluminate, $MgO{\cdot}Al_2O_3$)-bonded magnesia ceramic has been recognized as one of effective refractories in all parts of ladle furnaces, since Eusner and Hubble[9] first developed spinel-bonded magnesia-based bricks. As a substitute of carbon-bonding, $MgO{\cdot}Al_2O_3$ spinel offers a good improvement in both physical and chemical properties of MgO-based refractories, such as densification, slag penetration resistance, and thermal shock resistance.[10] A number of researchers have focused on the corrosion behavior between spinel-MgO and slag. Goto and coworkers[11] have found that $CaO\text{-}Al_2O_3\text{-}SiO_2$ slag penetrated into $MgO\text{-}MgO{\cdot}Al_2O_3$ spinel bricks could lead to the formation of secondary spinel, $CaMgSiO_4$, $Ca_3MgSi_2O_8$, and MgO as microscopic corrosion products. Recently, aluminum oxide as an addition was added into MgO-C refractory by Ganesh *et al*.[12,13] They found that refractories containing *in situ* spinel improved ceramic bonding and corrosion resistance. Some studies[14–16] have also been conducted to investigate the corrosion mechanism in the $MgO\text{-}Al_2O_3$ refractories. The factors including the pore size distribution, the change of liquid viscosity, and chemical reactions have been considered to evaluate the slag-refractory interaction. Besmann and Luz[17,18] have described the chemical reaction mechanisms between slag and refractory, as well as the changes in liquid slag composition after corrosion by thermodynamic calculation. However, the detailed analysis of microstructure and phase evolution by slag penetration has not been addressed sufficiently so far.

Despite many advantages of *in situ* spinel bonding, expansion difference between spinel and MgO is considered as one of the most serious drawbacks, which hinders the potential applications of this material. To control the expansion, the incorporation of finer particles in MgO-based refractory is one of the effective approaches. More recently, Braulio studied the effect of alumina particle size on controlling the expansion of alumina-magnesia refractories.[19,20] It was found that colloidal alumina suspension with nanoscale size presented the best performance.

In the present work, *in situ* spinel is formed by reaction between colloidal alumina and MgO matrix. The main purpose of the work is to investigate the

HUIJUN WANG, Graduate Student, BJÖRN GLASER, Senior Researcher, and DU SICHEN, Professor, are with Department of Materials Science and Engineering, Royal Institute of Technology, 10044 Stockholm, Sweden. Contact e-mail: sichen@kth.se
Manuscript submitted October 10, 2014.
Article published online January 6, 2015.

penetration behavior of ladle slag on MgO-*in situ* spinel substrates at 1873 K (1600 °C). The study focuses on the mechanism of the reaction between slag and refractory and the effect of the amount of alumina addition on slag penetration. The study is the first step to develop refractory for ladle line that can be used for the production of extra clean steel.

II. EXPERIMENTAL PROCEDURE

A. *Materials and Sample Preparation*

Coarse MgO powder (>98 pct purity) supplied by Sigma Aldrich was used as the matrix material. The particle size was 60 mesh (<300 μm) with a BET specific surface area of 2.82 m^2/g. Colloidal alumina suspension (50 pct in H_2O, 45 nm of average particle size) was used as addition to the MgO powder. The colloid was obtained from Alfa Aesar. To prepare the ceramic sample, MgO powder and colloidal alumina (the percentage corresponds to Al_2O_3 without H_2O) in desired proportions were mixed in a ceramic mortar for 1 hour. The mixture was uniaxially pressed into pellets (30 mm in diameter and 8 mm in thickness after sintering) using a stainless steel die under a pressure of 15 MPa. Thereafter, the pressed pellet was sintered at 1773 K in the muffle furnace with a heating rate of 3 K/min and 8 hour dwell. The total compositions of the prepared samples are listed in Table I.

In order to compare the properties of the prepared ceramic samples with the refractory used for ladle treatment, a commercial high-density MgO-C brick supplied by SSAB-Oxelösund was also studied. This type of refractory is usually used as the working lining of steelmaking ladles. Disks were cut out from the brick. In order to simulate the decarburized layer, the brick was pre-fired to burn out the graphite at 1373 K (1100 °C) for 10 hour. The brick after decarburization contained 97.2 mass pct MgO, 1.6 mass pct CaO, and traces of other oxides according to the supplier.

The materials used for slag along with their suppliers and purity levels are presented in Table II. All powders were dried at 1173 K (900 °C) for 10 h to remove moisture. The powders of CaO (55 mass pct), Al_2O_3 (30 mass pct), MgO (8 mass pct), and SiO_2 (7 mass pct) were mixed thoroughly in an agate mortar. The mixed powders were pressed into pellets (each about 2 g, 11 mm in diameter and 10 mm in thickness) and stored in a desiccator before being used in the experiment.

Table I. Chemical Compositions of the Ceramic Substrates

Type of Substrate	MgO (Mass Percent)	Colloidal Alumina (Mass Percent)
MS0	100	—
MS1	90	10
MS2	80	20

Table II. Supplier and Purities of Powders Used for Slag Preparation

Oxide	Supplier	Purity
CaO	Alfa Aesar	99.95 pct
Al_2O_3	Alfa Aesar	99.50 pct
MgO	Sigma Aldrich	>99 pct
SiO_2	Alfa Aesar	99.80 pct

B. *Setups*

To study the mechanism of reaction between molten slag and the ceramic substrates, a vertical furnace was used. The setup is schematically shown in Figure 1. The high-temperature furnace with super Kanthal heating elements was controlled using a B-type thermocouple (Pt-6 pct Rh/Pt-30 pct Rh). Another B-type thermocouple was placed just beneath the graphite sample holder. The alumina reaction tube was connected to a water-cooled quenching unit made of brass. The whole reaction chamber was sealed using O-rings. To ensure efficient quenching of the sample, the quenching unit had two gas inlets that enabled injection of argon gas with a high flow rate onto the sample when it was in the quenching position.

The sample was held in the graphite holder. Many holes were made in the holder to reduce its heat capacity. A graphite connecter connected the graphite holder to a long steel tube. The steel tube was placed in the central axial position and connected to the lift (driven by motor) above the reaction chamber. The steel tube could be moved both downward and upward by the lift, while the system was kept gas tight by O-rings. Fast quenching was enabled by moving the graphite holder from the hot zone of the furnace to the water-cooled quenching unit in less than one second using the lift.

For each run, the ceramic pellet (30 mm in diameter, 8 mm in thickness) was placed in the graphite sample holder with the slag pellet on its top. The sample was kept in the cooling chamber, when the reaction tube was

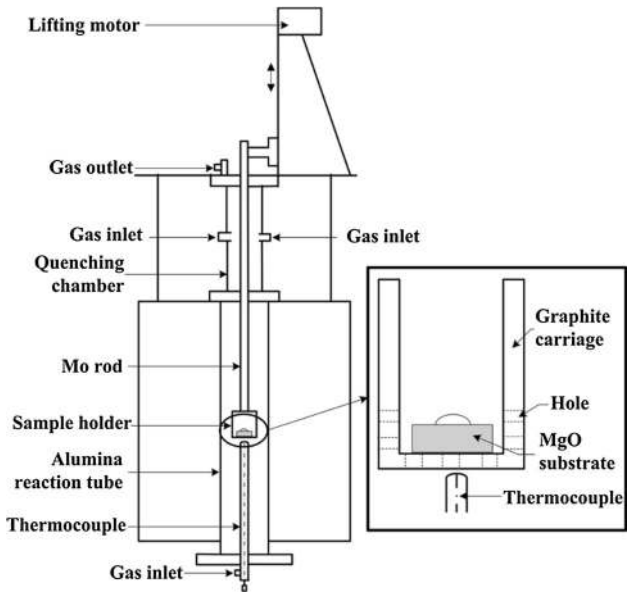

Fig. 1—Experimental setup.

evacuated, and then flushed with argon gas. The furnace was then heated up. When the furnace reached the target temperature, the sample was lowered down step by step into the hot zone of the furnace from the quenching chamber (in about 20 minute). Moving the sample slowly to the high temperature zone would avoid the thermal shock of the reaction tube, and at the same time reduce the reaction time between slag and substrate before melting of the slag. The slag was allowed to react with the ceramic pellet for a predetermined time, before the sample holder was rapidly lifted to the quenching chamber and quenched by high flow of argon gas.

All the experiments were repeated more than 2 times to examine the reproducibility of the results. In this study, the criteria to determine the reproducibility were the penetration depth, liquid composition, as well as the phase distribution at the grain boundaries.

C. *Analysis*

The bulk density and apparent porosity of the sintered ceramics MgO with different amounts of colloidal alumina were measured by the Archimedes method using water as an immersion medium. It should be mentioned that the hydration of MgO would affect the accuracy of the apparent porosities and bulk densities when water was used as immersion medium due to the possible formation of $Mg(OH)_2$. However, in view that the samples were sintered at high temperature and the density measurements in the water were fast, the uncertainty introduced by MgO hydration could be expected relatively small to affect the discussion. X-ray diffraction (XRD) analysis was carried out using a Bruker D8 Advance X-ray diffractometer (Karlsruhe, Germany; Cu K_α radiation generated at 40 kV and 40 mA), with 2θ ranging from 10 deg to 80 deg and a scanning speed of 6 deg/min. The microstructure and chemical composition of the specimen were determined by a scanning electron microscope (SEM, Hitachi TM3100, Japan) with an energy dispersive spectroscopy (EDS) analyzer.

III. RESULTS

A. *MgO-In Situ Spinel Substrates*

The X-ray diffraction patterns of sintered MgO substrates with different amounts of colloidal alumina addition are shown in Figure 2. Because of the chemical reaction between MgO and Al_2O_3 during the sintering, the second phase, spinel is formed. As seen in the figure, in the absence of Al_2O_3 addition, only MgO phase is present. On the other hand, both MS1 and MS2 samples consist of two phases, namely MgO and spinel. The figure also shows that an increase of the colloid addition results in an increase of the intensity of the spinel peak.

SEM and EDS analyses were conducted to show the morphology of *in situ* spinel in the MgO matrix, and to examine its composition. The SEM images of the sintered MS0, MS1, and MS2 are presented in Figures 3(a) through (c), respectively. The sample of MS0

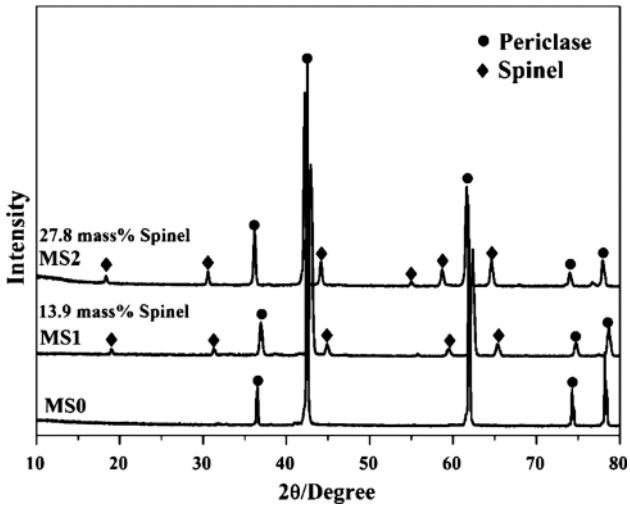

Fig. 2—X-ray diffraction patterns of MgO substrates with different amounts of colloidal alumina addition.

without colloidal alumina addition was much more porous than MS1 and MS2. A large amount of open pores can be seen in the matrix of MgO grains. MgO grains of sample MS2 showed the normal equiaxed morphology, while MS0 was sphere-like. Small spinel grains as a second phase located at the grain boundaries of MgO are observed in the samples of MS1 and MS2 (see Figures 3(b) and (c)). To obtain a clear morphology of spinel grains, fracture microstructure without surface polishing is inserted in Figure 3(c). It can be seen that classic octahedral spinel grains, sizing 2 to 4 μm, grow up around magnesia grains. The element mapping of Al is presented in Figure 3(d) for MS2. Al element is distributed uniformly in the Mg matrix. From Table III, EDS analysis reveals an element ratio 30.6/69.4 of the two oxides in the spinel phase. This ratio is quite near the stoichiometric $MgAl_2O_4$. The apparent porosities and bulk densities of MgO with different amounts of colloidal alumina addition are listed in Table IV. A density increase is observed with the increase of colloidal alumina addition, which corresponds with the porosity decrease. The difference in porosity confirms that the spinel formation plays a crucial role in ceramic bonding. It should be mentioned that the pore size would also have important impact on the slag infiltration. However, MgO substrates without addition of colloidal alumina and industrial MgO refractory with decarburization have a very porous structure. It consists of a large amount of "interconnected" irregular open pores. It is very difficult to obtain the accurate distribution of pore sizes. In Table IV, the obvious difference in porosity is intended to show relatively the role of colloidal alumina addition.

B. *Slag Penetration*

The penetration profiles of the three substrates after wetting tests of 30 minute at 1873 K (1600 °C) are shown in Figure 4. As indicated by the markers, slag has penetrated through MgO matrix to different depths. In

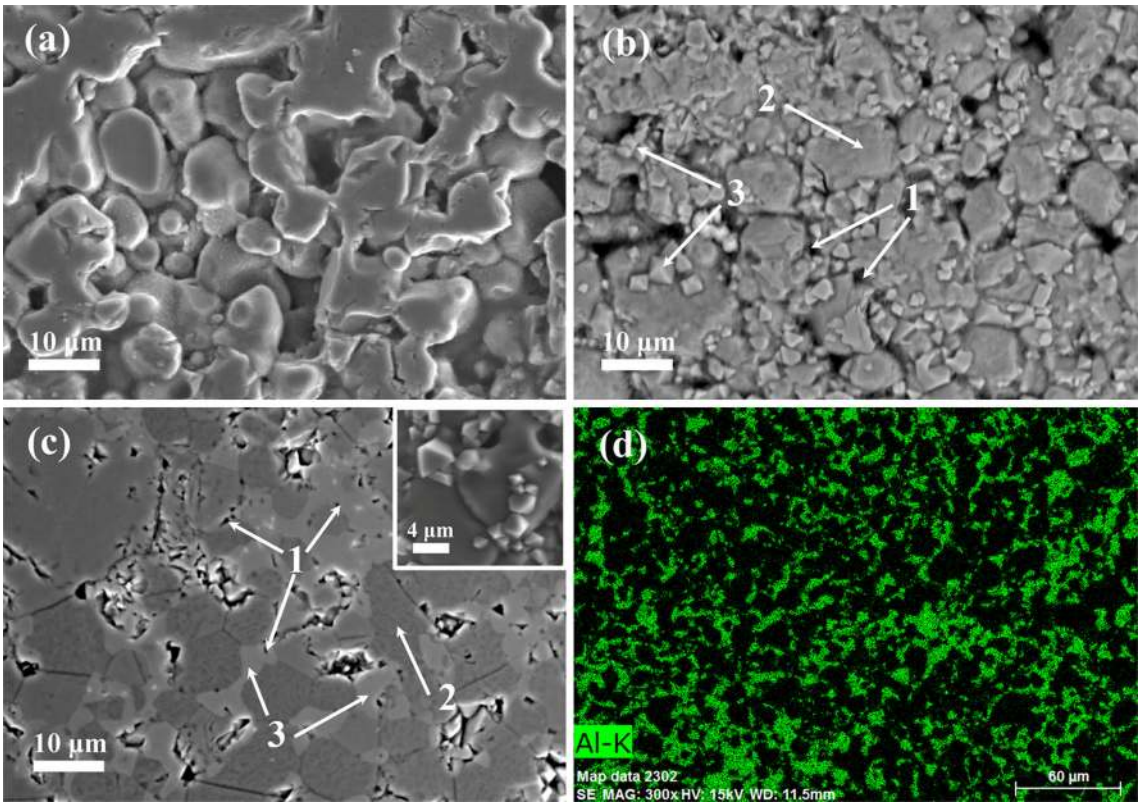

Fig. 3—SEM images of the samples; (*a*) MS0, (*b*) MS1, (*c*) MS2, and (*d*) element mapping of Al in sample MS2; Pores marked as 1, MgO marked as 2, and Spinel marked as 3.

Table III. Elements Composition of Mg/Al for Spinel Phases

Element	Series	Norm. C (Weight Percent)	Atom. C (Atomic Percent)
Magnesium	K-series	28	31
Aluminum	K-series	72	69

Table IV. Apparent Densities and Porosities of MgO with Different Amounts of Alumina Addition

Sample No.	Density (g/cm^3)	Porosity (Percent)
MS0	2.343	34.25
MS1	2.780	19.74
MS2	2.899	16.63

both cases of MC and MS0, the components of the slag have reach the bottom of the pellet, while in the case of MS1 and MS2, the slag has penetrated to the levels of 6.5 and 4 mm, respectively, from the upper surface of the pellet. The results reveal that the addition of colloidal alumina (as a consequence, the formation of the spinel phase) helps to limit the slag penetration into the MgO matrix. Detailed discussion about the depth of slag penetration and microstructure is given in the later sections.

The samples after the experiments in the vertical furnace are subjected to SEM and EDS analyses. The substrate is divided into 4 zones equally from the top to bottom (each zone is 2 mm). To help the discussion, these zones are named as A, B, C, and D from the top to the bottom.

The phases present in the 4 zones are identical in the reacted MS0 substrate. For brevity, only the SEM microphotograph of Zone D of the MS0 sample is presented in Figure 5. Beside the MgO matrix, two phases are found at the grain boundaries of the MgO phase throughout the whole thickness, namely phase 2 and phase 3. Note that only small amount of phase 3 is seen in the sample, while the amount of phase 2 is relatively big. According to EDS analysis, phase 2 has a composition of 1 to 3 mass pct MgO, 38 to 41 mass pct Al_2O_3, and 56 to 59 mass pct CaO. The composition of this phase (in the liquid region as indicated by the phase diagram[21]) and the fact that it fills up the MgO grain boundaries indict this phase being liquid at the experimental temperature. Phase 3 has a composition close to $12CaO{\cdot}7Al_2O_3$. An examination of the phase diagram of the binary $CaO\text{-}Al_2O_3$[21] suggests that $12CaO{\cdot}7Al_2O_3$ is likely to precipitate from molten slag during quenching, since the melting temperature of this phase is below 1873 K (1600 °C). Note that the content of MgO in the liquid phase was lower than initial slag composition. Besides, SiO_2 content after each test has decreased considerably. The amount of Si element is hardly to detect in the penetrated slag. One plausible explanation for the low MgO content and low SiO_2 content in the infiltrated slag is the low oxygen potential in the system. The oxygen potential employed is very close to that

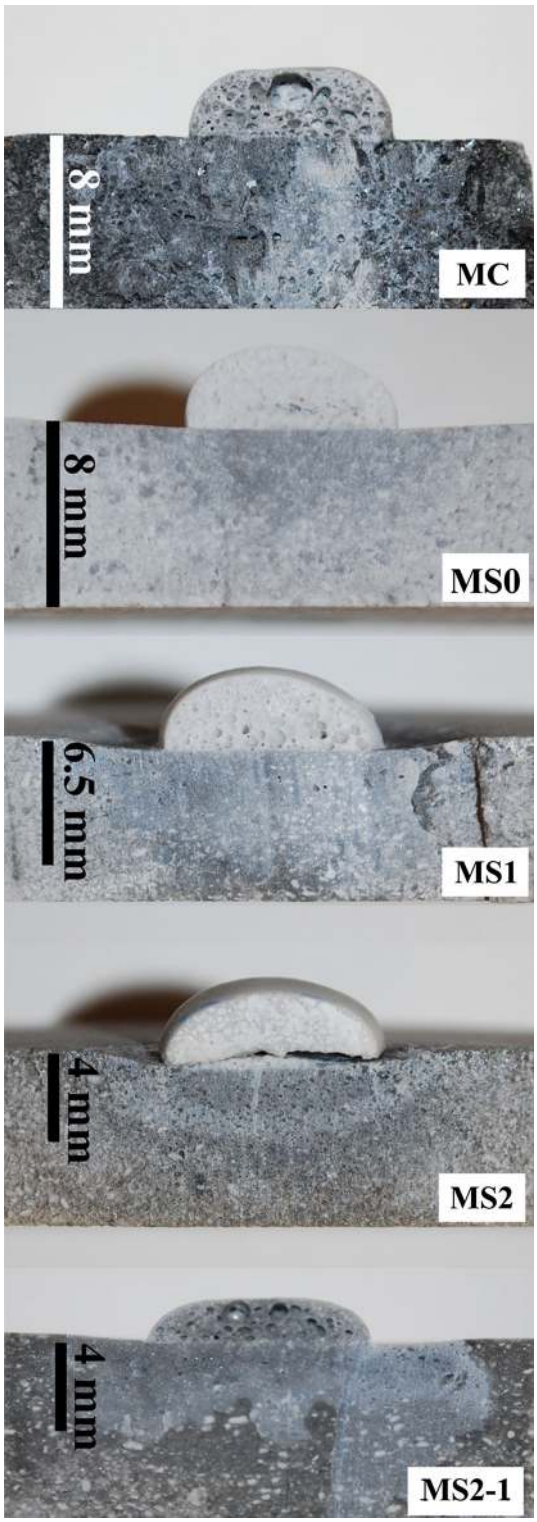

Fig. 4—Penetration profiles after the tests.

prevailing in a ladle furnace, about $P_{O2} = 10^{-16}$ atm. The formation of Mg gas and SiO gas at such low oxygen potential would well explain the loss of both MgO at the surface and SiO_2 in the slag.

The phases found in MS1 and MS2 samples after reaction vary with the position of the zone. As an example, Figures 6(a) through (d) present the SEM

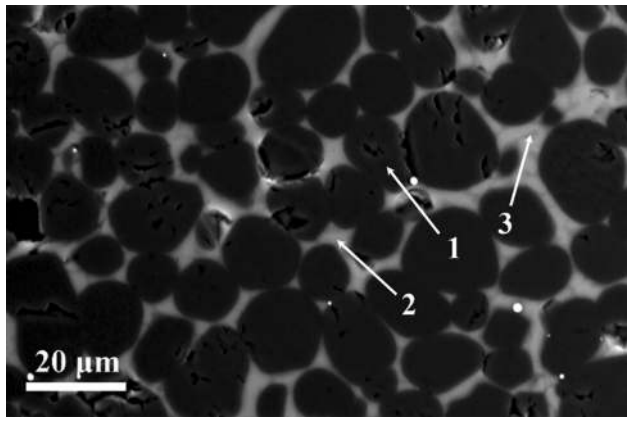

Fig. 5—SEM image of MS0 substrate in Zone D; MgO matrix marked as 1, liquid phase marked as 2, and $12CaO{\cdot}7Al_2O_3$ marked as 3.

microphotographs of Zones A, B, C, and D in the reacted MS2 substrate. In Zone A, the phases present are identical to the phases in the substrate MS0. The MgO grains in the matrix are surrounded by two phases, which are identified as $12CaO{\cdot}7Al_2O_3$ and liquid phase.

As the slag penetrates deeper (Zone B, see Figure 6(b)), the continuous liquid phase is still the major phase at the grain boundaries. It is worthwhile to mention that the content of Al_2O_3 in the liquid phase has increased comparing to the liquid in Zone A. The composition of the liquid is about 5 to 7 mass pct MgO, 42 to 45 mass pct Al_2O_3 and 50 to 52 mass pct CaO. The increased content of Al_2O_3 is because of the dissolution of *in situ* spinel into the liquid. Small amount of spinel grains (phase 4) is found around the MgO matrix. Besides, tiny pieces of $CaO{\cdot}Al_2O_3$ (CA) phase (1 to 2 μm) are detected on the surface of "unreacted" spinel grains, marked as 5.

When the liquid slag goes down into Zone C, there is a clear difference in the phase distribution. Instead of liquid phase filling up the grain boundaries, solid phases occupy most of spaces among MgO grains (Figure 6(c)). In this zone, liquid phase is a minor phase surrounding the solid pieces. In comparison with Zone B, more spinel grains are seen in this zone, suggesting that less spinel has dissolved into the liquid phase in this zone. The major phase at the grain boundaries is the light gray $CaO{\cdot}Al_2O_3$ phase that formed as a continuous, adherent layer on the spinel surface. While the liquid phase is descending through the MgO matrix, the spinel phase is dissolved into the liquid. The dissolution of spinel increases the contents of both Al_2O_3 and MgO in the liquid. As indicated by the phase diagram,[21] the increase of Al_2O_3 will lead to the precipitation of the $CaO{\cdot}Al_2O_3$ phase at 1873 K (1600 °C). At the same time, the dissolution of the spinel phase is also stopped due to the increase of the activities of Al_2O_3 and MgO in the liquid. It is interesting to mention that a few round darker grains are found in Zone C. These grains are identified as $CaO{\cdot}MgO{\cdot}Al_2O_3$ (CMA) solid solution (marked as phase 6). The presence of the $CaO{\cdot}MgO{\cdot}Al_2O_3$ phase is also explained by the phase diagram of the Al_2O_3-CaO-MgO ternary.

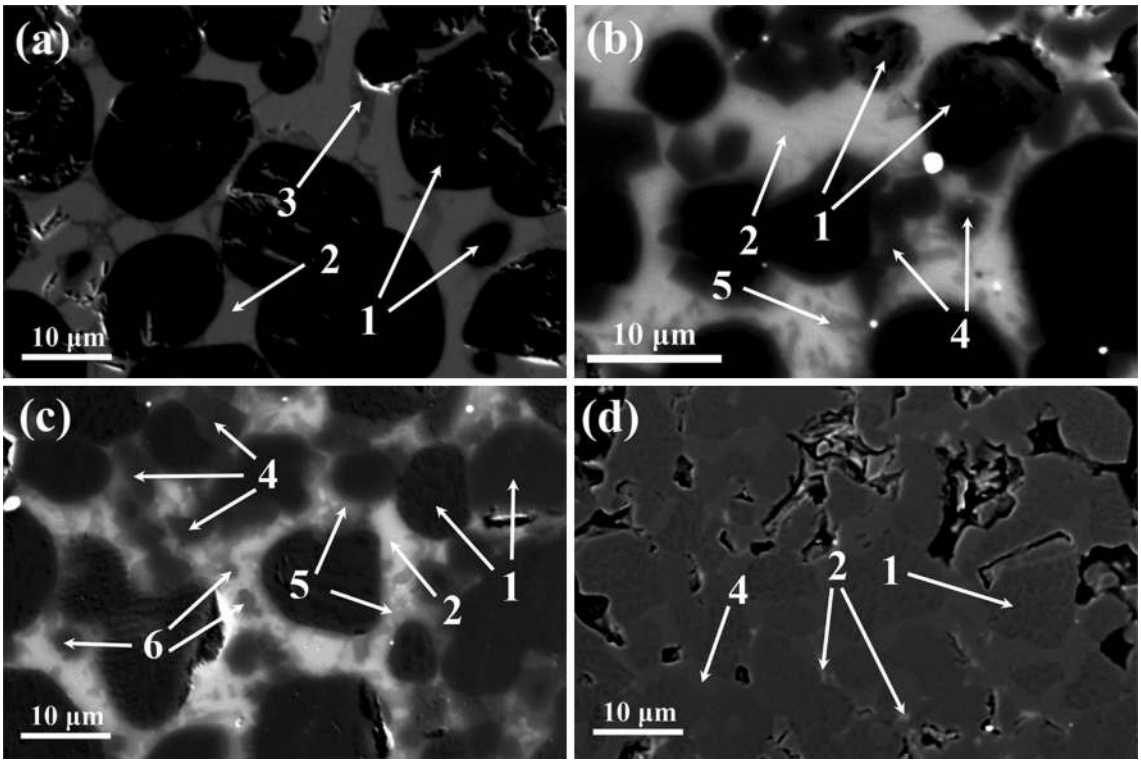

Fig. 6—SEM image of MS2 in (*a*) Zone A, (*b*) Zone B, (*c*) Zone C, and (*d*) Zone D; MgO matrix marked as 1, liquid phase marked as 2, $12CaO{\cdot}7Al_2O_3$ marked as 3, spinel as 4, $CaO{\cdot}Al_2O_3$ as 5, and CMA solid solution marked as 6.

In Zone D, the bottom region of the substrate, the slag penetration is absent. As shown in Figure 6(d), only the MgO and spinel phases are detected. The morphology of this zone is very similar as the substrate before reaction shown in Figure 3(c). The phase distributions in Figures 6(a) through (d) show evidently the formation of the solid phases ($CaO{\cdot}Al_2O_3$ and $CaO{\cdot}MgO{\cdot}Al_2O_3$) due to the saturation of Al_2O_3 in the liquid phase at the grain boundaries. The precipitation of the solid phases would block the open pores of the substrate finally. This would stop further slag penetration.

Table V summarizes the phases found in grain boundaries of different zones after the experiments. In the table, MC stands for the substrate cut out from a brick of carbon bearing MgO refractory for the use in ladle lining. After 30 minute, slag has penetrated into the refractory through the entire thickness of the sample, as seen in Figure 4(MC). The phases present in each zone after reaction are identical as the ones found in the reacted MS0 substrate. This aspect is exemplified by the phases in Zone D shown in Figure 7. It should be pointed out the comparison between the industrial bricks and the sintered dense samples should be used with precaution. Real comparison should be made only when the two samples have similar grain sizes of the MgO particles and similar porosities. This would be the topic in the coming study.

To examine whether the reacted layer in the reacted MS2 substrate can further help to block the slag penetration in the next heat of the ladle treatment, experiment of MS2-1-Run1 was conducted. In this experiment, the substrate of type MS2 was first reacted with slag with the same experimental condition as MS2-Run1. The substrate was used again to react with new slag in a new experiment.

The double penetration on MS2-1-Run1 did increase the corrosion area, but only in the horizontal direction. Comparison of the two samples indicates that the increase of penetration in depth is negligible (shown by SEM analysis). In view that the ladle is used for many heats, this double penetration experiments are very necessary. For the same reason, the focus is given to the depth of the slag attract in the case of double penetration experiments. Only traces of liquid phase (almost negligible) are detected in Zone D in the sample. In this zone, the major phase at the grain boundaries is spinel.

IV. DISCUSSION

As shown in Table V, all the experiments are repeated. The results are reproducible. In fact, in most cases, the experiments are repeated a few times.

A. *Slag Penetration*

As shown in Figure 3(a), there is a considerable amount of open pores left in the substrate. The probable cause of the case is the poor sinterability of coarse MgO powders. The addition of colloidal alumina has positive effect on the densification as revealed by the results in Table IV. This finding is in agreement with the observation by Ghosh *et al.*[9,22,23] This can be attributed to

Table V. Phases Found at the Grain Boundaries of MgO After Reaction

Substrate	Test	Zone	Amount of Liquid Phase	Spinel	$CaO{\cdot}Al_2O_3$	CMA
MS0	Run1	A	major	—	—	—
		B	major	—	—	—
		C	major	—	—	—
		D	major	—	—	—
	Run2	A	major	—	—	—
		B	major	—	—	—
		C	major	—	—	—
		D	major	—	—	—
MS1	Run1	A	major	—	—	—
		B	major	—	—	—
		C	major	yes	—	—
		D	minor	major	yes	—
	Run2	A	major	—	—	—
		B	major	—	—	—
		C	major	yes	—	—
		D	minor	major	yes	—
MS2	Run1	A	major	—	—	—
		B	major	minor	yes	—
		C	minor	major	minor	yes
		D	—	major	—	—
	Run2	A	major	—	—	—
		B	major	minor	yes	—
		C	minor	major	minor	yes
		D	—	major	—	—
MS2-1	Run1	A	major	—	—	—
		B	major	minor	yes	—
		C	minor	major	minor	—
		D	trace	major	—	—
	Run2	A	major	—	—	—
		B	major	minor	yes	—
		C	minor	major	minor	—
		D	trace	major	—	—
MC	Run1	A	major	—	—	—
		B	major	—	—	—
		C	major	—	—	—
		D	major	—	—	—
	Run2	A	major	—	—	—
		B	major	—	—	—
		C	major	—	—	—
		D	major	—	—	—

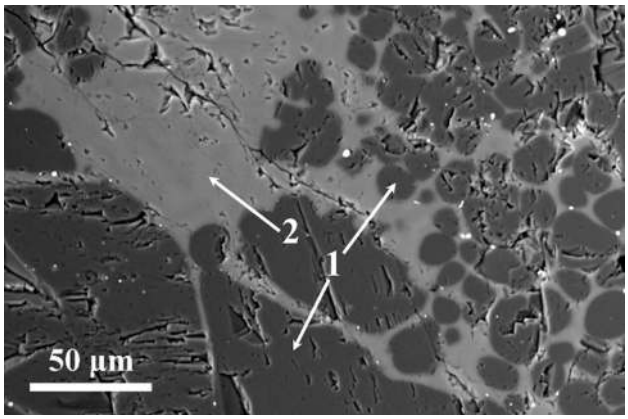

Fig. 7—SEM image of MC substrate in Zone D; MgO matrix marked as 1, liquid phase marked as 2.

the formation of *in situ* spinel phase. Small spinel grains as the second phase fill up the inter-granular gaps (or open pores) between magnesia grains, playing a role of an excellent ceramic bonding. This bonding contributes to dense structures with lower porosity. Another aspect that also makes contribution to the densification is the tiny size of the Al_2O_3 particles in the colloidal suspension. Finer particles of alumina could enhance the MgO-Al_2O_3 inter-diffusion driving force; and moreover, colloidal suspension could lower self-agglomeration.[19,24]

In the case of commercial carbon bearing MgO refractory, the liquid slag is the primary phase at the grain boundaries. In general, the slag penetrating depends on the physical properties of substrates, such as apparent porosity, grain boundaries, cracks, *etc.*[25] In MgO refractory, large amounts of open pores are the main channels of slag penetration. Capillary sucking

pressure is the major driving force for the infiltration of the liquid. Although the grain size of MgO particles in MS0 samples is somewhat different from that of the industrial refractory MC, the same behavior of slag penetration is observed. Even the phases found among the MgO grains are identical in these two cases. It could be expected that the present finding would throw some lights on the development of new refractory materials for making clean steel. For example, colloidal alumina could be used to replace carbon as additives in industrial MgO refractory. However, a good refractory based on MgO should also have improved mechanical properties and be economically sound. These aspects would need further detailed studies (which is currently carried out in the present group).

As already mentioned in the introduction part, ladle glaze is a very important source of the formation of inclusions.[1–8] When the top slag goes down following the steel during the draining of the ladle, it adheres to the ladle lining. The adhered slag penetrates into the open pores of the MgO refractory. This phenomenon is well demonstrated by the present experimental results with MS0 and MC samples. The slag-infiltrated layer would not be easily removed because of the MgO matrix. In the next heat, the movement of the liquid steel near the wall would flush off pieces of the slag-infiltrated layer resulting in macro calcium aluminate inclusions.[5,8]

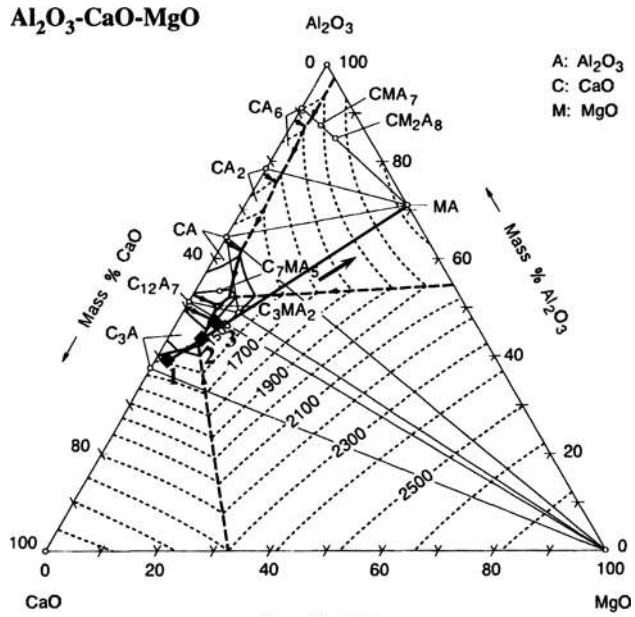

	Point 1	Point 2	Point 3
MgO	1.8	6.2	6.3
Al_2O_3	39.5	43.1	46.8
CaO	58.7	50.7	46.9

Fig. 8—CaO-Al_2O_3-MgO phase diagram with the compositions of the liquid phase found in different zones of the MS2 substrate.

B. *Effect of Colloidal Alumina Addition*

As discussed in the result part, the addition of 20 mass pct colloidal alumina can efficiently limit the slag penetration. The increased resistance to slag penetration by spinel formation is in good agreement with the observation of Ganesh *et al.*[12] As seen in Table V, very little amount of liquid phase is observed 4 mm away from the slag-MS2 interface. A lot of spinel particles are still found in Zone C after reaction of 30 minute. In Zone D, no liquid phase is detected. The morphology of Zone D is more or less the same as the prepared ceramic. Putting the reacted substrate into contact again with new slag does not show serious slag penetration (MS2-1-Run1). In Zone D of the doubly used substrate, no liquid phase is seen. It is evident that adding colloidal alumina into MgO has a positive effect on penetration resistance. The suppressed penetration of slag could be partly due to the improvement of the microstructure of the substrate, since the decreased porosity by spinel bonding could lead to the reduction of sucking pressure.[13] The presence of Al_2O_3 in the spinel phase plays another important role in improving the penetration resistance. This role is evidently brought out by the variation of phases in different zones of the reacted substrate, MS2 (even MS1). To elaborate the discussion, the average compositions of the liquid phase in different zone of reacted MS2 are presented in the Al_2O_3-CaO-MgO phase diagram[21] (Figure 8). The dissolution of the spinel phase (MA) results in the increase of the contents of Al_2O_3 and MgO. This aspect is clearly shown by the fact that the composition of the liquid moves toward MA, as the slag penetrates through the substrate. It is evident that the local thermodynamic equilibrium varies with the depth of the penetration. The dissolution of MA would finally lead to the vanishing of the liquid phase and the formation of $CaO{\cdot}Al_2O_3$ and even CMA solid solution. Note that both the melting temperatures of CA and CMA solid solution are above 1873 K (1600 °C). The formation of the solid phase(s) would completely block the pores and stop further slag penetration. It is likely that the presence of *in situ* spinel would slow down mechanically the penetration of the liquid phase, therefor giving time for the liquid phase to react with the substrate component (in the present case the spinel phase). However, the most profound contribution of spinel phase is its dissolution into the liquid, leading finally the vanishing of the liquid phase.

When the liquid slag has just penetrated into the substrate, the main mechanism of the reaction between slag and refractory would be the dissolution of spinel into liquid phase. When more and more spinel has dissolved into the liquid slag as the liquid penetrating, the liquid phase would be saturated by spinel. Further reaction of the liquid phase and MA leads to the formation of other solid phase(s) and finally vanish of the liquid. The blocking effect by the presence of spinel particles at the MgO grains functions even when new slag is used. This aspect is evidently brought out by the result of MS2-1-Run1, where the reacted MS2 substrate is reacted with fresh slag in the second run. The phase distribution with the depth is very similar to the "one-time" (MS2-Run1) penetration. This means that those solid phases which have been formed previously become

the "real" barriers to inhibit the slag penetration. It should be pointed out that the change of viscosity of the oxide liquid could have certain influence on the penetration and corrosion. It is very difficult to identify the contribution of the formation of solid particles and the increased viscosity on the inhabitation of slag penetration. Nevertheless, it is expected that when the fraction of solid phase increases, the contribution of solid phase would be dominating. It is also interesting to mention that the viscosity of basic ladle slag has actually negligible effect on the formation of inclusions from the lining in the ladle.[26] Table V also indicates that the amount of addition of colloidal alumina is essentially important. Addition of 10 mass pct has much less impact on the resistance of slag penetration, while 20 pct addition leads to substantial improvement.

The present result suggests a potential approach to generate new MgO-based refractory for making clean steel. However, the results should only be considered as preliminary. The following aspect must be carefully studied. (1) Using much coarser grains of MgO to verify the applicability of the new approach. (2) The applicability of the material with respect to the mechanical properties must be studied. (3) The amount of addition of colloidal alumina needs to be further examined. (4) The interaction between the refractory and steels with different compositions needs to be investigated.

V. SUMMARY

MgO-*in situ* spinel substrates were prepared by sintering the mixtures of coarse MgO and colloidal alumina at 1773 K (1500 °C) for 8 hour. $MgAl_2O_4$ spinel phase was formed during sintering in the substrates. The presence of spinel phase decreased the porosity of substrates. Addition of 20 mass pct colloidal alumina into MgO substrate showed a porosity of 16.6 pct.

In situ spinel was found to have positive effect on the resistance of slag penetration. Addition of 20 mass pct colloidal alumina could greatly limit the slag penetration into the MgO substrate. The suppressed penetration of slag could be partly due to the decreased porosity by spinel bonding which led to the reduction of sucking pressure. The presence of Al_2O_3 in the spinel phase played another important role in improving the penetration resistance. The dissolution of the spinel phase resulted in the increase of the contents of Al_2O_3 and MgO in the liquid oxide phase. The formation of solid oxide phases, $CaO{\cdot}Al_2O_3$ and $CaO{\cdot}MgO{\cdot}Al_2O_3$ at the grain boundaries would create the barriers to hinder further penetration. The results suggested a possible solution to improve the resistance of MgO-based refractory to produce steel having good cleanness.

ACKNOWLEDGMENT

The authors are thankful for the financial support of China Scholarship Council in the form of scholarship to the first author.

REFERENCES

1. G.J. Hassall, K.G. Bain, N. Jones, and M.O. Warman: *Ironmak. Steelmak.*, 2002, vol. 29, pp. 383–89.
2. S. Riaz, K.C. Mills, and K. Bain: *Ironmak. Steelmak.*, 2002, vol. 29, pp. 107–13.
3. K. Beskow, J. Jia, C.H.P. Lupis, and D. Sichen: *Ironmak. Steelmak.*, 2002, vol. 29, pp. 427–35.
4. K. Beskow and D. Sichen: *Ironmak. Steelmak.*, 2004, vol. 31, pp. 393–400.
5. K. Beskow and N. Sano: *Iron Steel Technol.*, 2006, vol. 3, pp. 103–17.
6. C.W. Bale, P. Chartrand, S.A. Degterov, G. Eriksson, K. Hack, R. Ben Mahfoud, J. Melançon, A.D. Pelton, and S. Petersen: *CALPHAD*, 2002, vol. 26, pp. 189–228.
7. I.H. Jung, J.H. Son, S.M. Jung, H. Gaye, and H.G. Lee: *Proceedings ICS 2008: The 4th International Congress on the Science and Technology of Steelmaking*. 2008. pp. 395-98.
8. M. Song, M. Nzotta, and D. Sichen: *Steel Res. Int.*, 2009, vol. 80, pp. 753–60.
9. G.R. Eusner and D.H. Hubble: *J. Am. Ceram. Soc.*, 1960, vol. 43, pp. 292–97.
10. S. Zhang and W.E. Lee: *Spinel-containing Refractories, Refractories Handbook*, Marcel Dekker Inc., New York, 2004, pp. 215–58.
11. K. Goto, B.B. Argent, and W.E. Lee: *J. Am. Ceram. Soc.*, 1997, vol. 80, pp. 461–71.
12. I. Ganesh, S. Bhattacharjee, B.P. Saha, R. Johnson, K. Rajeshwari, R. Sengupta, M.V. Ramana Rao, and Y.R. Mahajan: *Ceram. Int.*, 2002, vol. 28, pp. 245–53.
13. M. Bavand-Vandchali, F. Golestani-Fard, H. Sarpoolaky, H.R. Rezaie, and C.G. Aneziris: *J. Eur. Ceram. Soc.*, 2008, vol. 28, pp. 563–69.
14. M.K. Cho, G.G. Hong, and S.K. Lee: *J. Eur. Ceram. Soc.*, 2002, vol. 22, pp. 1783–90.
15. M.A.L. Braulio, A.G. TombaMartinez, A.P. Luz, C. Liebske, and V.C. Pandolfelli: *Ceram. Int.*, 2011, vol. 37, pp. 1935–45.
16. L.A. Díaz, R. Torrecillas, A.H. de Aza, and P. Pena: *J. Eur. Ceram. Soc.*, 2007, vol. 27, pp. 4623–31.
17. T.M. Besmann: *CALPHAD*, 2008, vol. 32, pp. 466–69.
18. A.P. Luz, A.G. Tomba Martinez, M.A.L. Braulio, and V.C. Pandolfelli: *Ceram. Int.*, 2011, vol. 37, pp. 1191–201.
19. M.A.L. Braulio, M.F.L. Piva, G.F.L.E. Silva, and V.C. Pandolfelli: *J. Am. Ceram. Soc.*, 2009, vol. 92, pp. 559–62.
20. M.A.L. Braulio, G.G. Morbioli, L.R.M. Bittencourt, and V.C. Pandolfelli: *J. Am. Ceram. Soc.*, 2010, vol. 93, pp. 2606–10.
21. V. D. Eisenhüttenleute: *Slag Atlas.*, Verlag Stahleisen GmbH, 1995.
22. A. Ghosh, R. Sarkar, B. Mukherjee, and S.K. Das: *J. Eur. Ceram. Soc.*, 2004, vol. 24, pp. 2079–85.
23. K. Gotod and W.E. Lee: *J. Am. Ceram. Soc.*, 1995, vol. 78, pp. 1753–60.
24. M. Nouri-Khezrabad, M.A.L. Braulio, V.C. Pandolfelli, F. Golestani-Fard, and H.R. Rezaie: *Ceram. Int.*, 2013, vol. 39, pp. 3479–97.
25. W.E. Lee and S. Zhang: *Int. Mater. Rev.*, 1999, vol. 44, pp. 77–104.
26. M. Song, M. Nzotta, and D. Sichen: *Ironmak. Steelmak.*, 2011, vol. 38, pp. 584–89.